NUMERICAL SIMULATION OF THE HEAT PENETRATION IN TWO-PLATE ARC WELDING

C. Payares[1], L. Rojas-Solórzano[2], P. Viggiani[3]

(1) Departamento de Mecánica, Universidad Simón Bolívar, Venezuela. email: cpayares@usb.net
(2) Departamento de Conversión de Energía, Universidad Simón Bolívar, Venezuela. email: rrojas@usb.net
(3) Departamento de Mecánica, Universidad Simón Bolívar, Venezuela. email: viggiani@usb.net

ABSTRACT

A mathematical model and numerical simulation of the three-dimensional and transient metal arc-welding process is presented. The heat source is considered as spatially distributed following a centered Gaussian bell, while the substract material (Al 6063) is assumed homogeneous and isotropic with temperature-dependent thermal properties. Radiation and convection are also calculated through an empirical temperature-dependent correlation. Phase-change phenomenon is included as a discontinuity in the material specific heat. Calculations were performed by using a finite volume code (CFX4.2™). Computed heat penetration and weld metal area are found to be in good agreement with experimental data.

INTRODUCTION

Metal arc-welding is one of the most popular manufacturing processes in industry. This manufacturing process is widely used in the fabrication of: ships, nuclear reactors, bridges, automobiles, trains, pressure vessels, etc. In all those applications, safety and economy are important concerns and therefore, large amounts of money and time are usually invested in developing empirical relationships[1] to describe the interaction among all relevant process variables (i.e., voltage, current intensity, welding speed and arc-length) and their influence onto the weld average dimensions (resistance).

Despite substantial effort, results from experimental studies are currently useful for applications within the explored range of the operating parameters. Changes in the material composition, plate width or another process variable, would imply the necessity of new experiments to derive the properly fitted equations. Therefore, numerical simulation is gaining more and more importance in today's investigation of the welding process.

In the study of the arc-length welding process, temperature profiles are of primary relevance since, for a given material and joint design, the temperature distribution determines the: (a) size of melted region; (b) heat-affected area; (c) resultant microestructure and associated mechanical properties; (d) residual stresses; and (d) plastic deformation of substract plate.

The computed results permits to co-relate the process input variables (i.e., voltage, current intensity, welding speed, etc.) and the final effects (numerated above) in a shorter time-scale, more versatile and a less expensive procedure than found by experimental means.

MATHEMATICAL MODEL

Figure 1 shows the schematics of the plate-to-plate butt-welding process using arc welding. The heat source (plasm arc) moves along the upper surface above the two plates interface, at a constant velocity V.

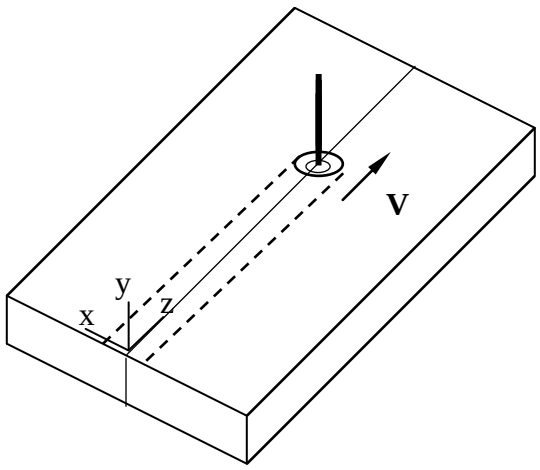

Figure 1. Schematics of the arc-welding process

The two-plate butt-welding problem is modeled as a heat source applied along the z-axis translating at a constant speed. The governing equation is the energy equation, given in cartesian coordinates as:

$$\frac{\partial}{\partial x}\left(Kx\frac{\partial T}{\partial x}\right)+\frac{\partial}{\partial y}\left(Ky\frac{\partial T}{\partial y}\right)+\frac{\partial}{\partial z}\left(Kz\frac{\partial T}{\partial z}\right)+Q = \rho Cp\frac{\partial T}{\partial t} \quad (1)$$

where,

T: Temperature
K: Thermal conductivity
Q: Heat source intensity per unit volume
ρ: Density
Cp: Specific heat
x,y,z: spatial coordinates referred to a fixed-to-plate reference system.

The material thermal properties (i.e., K and Cp) are considered as temperature dependent, homogeneous and isotropic. Figure 2 shows K and Cp values used in the simulations (taken from ref. [2]). The analysis neglects the internal heat dissipation due to eddy currents associated to the arc-weld magnetic field.

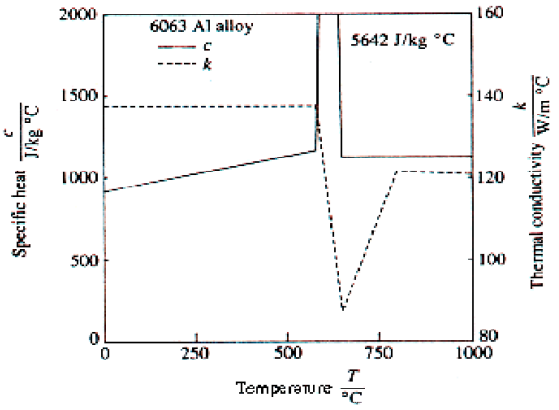

Figura 2. Thermal conductivity and specific heat as a function of temperature for aluminum alloy AL 6063

Boundary conditions

Symmetry along the z-axis leads to:

$$\frac{\partial T}{\partial x} = 0 \text{, at x = 0} \qquad (2)$$

Gauss-bell-like heat source, shown in Fig. 3, over upper surface, given by [3]:

$$q(x,\xi) = \frac{3.Qo}{\pi.r_b^{\,2}} \exp(-3.(x^2+\xi^2)/r_b^{\,2}) \qquad (3)$$

where,

$$\xi = z + V(\tau - t) \qquad (4)$$

$$Qo = \eta.E.I \qquad (5)$$

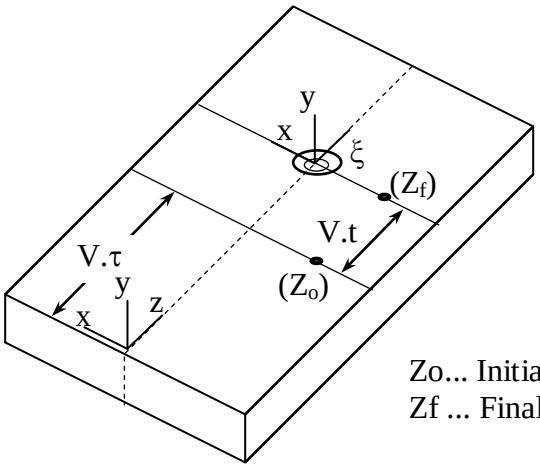

Zo... Initial position of the source (t = 0)
Zf ... Final position

Figure 3. Computational reference coordinate system

where,

Qo: Energy out of the electrode
r_b: Arc-weld effective radius, where 95% of Qo is effectively applied
η: Electrode overall efficiency
E: Arc-weld voltage
I: Arc-weld electric current
t: Time
τ: Position of heat source at t = 0
V: electrode translation speed

Sometimes, for the sake of clarity, it is convenient to express the heat source equation in x,y,z-coordinates. Thus, eqn. (3) becomes:

For $x^2 + \xi^2 < r_b^2$,

$$q(x,z,t) = \frac{3.Qo}{\pi.r_b^{\,2}} \exp(-3.(x^2 + (z + V(\tau - t))^2) / r_b^{\,2}) \qquad (6)$$

And, for $x^2 + \xi^2 \geq r_b^2$,

$$q(x,z,t) = 0 \qquad (7)$$

On the upper side of the plate, outside the disc of radius r_b, and within the rest of the surfaces, but the lower side, there is heat flux leaving the metal sheet, due to convection and radiation, given by:

$$q_{eff} = -h_{eff} (T_s - T_{inf}) \qquad (8)$$

where,

h_{eff}: effective heat transfer coefficient (considers convection and radiation) ($W/m^2.K$) [4]

$$h_{eff} = 0{,}00241.\varepsilon.T_s^{\,1.61} \qquad (9)$$

where,

ε: Material emissivity

T_s: Surface temperature

T_{inf}: Surrounding temperature

On the lower side, the temperature gradient in y-direction is zero:

$$\frac{\partial T}{\partial y} = 0 \qquad \text{for y = -e} \qquad (10)$$

where,

e: Metal sheet thickness

Latent (Fusion) heat

Latent heat, ΔH_f, is modeled as a singularity in the metal specific heat equation [5]:

$$Cp = Cp(T) + \Delta H_f \delta(T_S - T_{liq}) \qquad (11)$$

where,

Cp(T): Non-singular function

δ: Delta de Dirac function

Experimental Setup and Procedure

Aluminum 6063 T5 test probes, 6.35 mm thick, 50.8 mm wide and 80 mm long, were designed. Plate-to-plate butt-welding were made on flat faces without gap between. The welding process was performed in horizontal position, using electrodes type ER5356 (see Table 2) and Argon 100% pure as the protective gas.

Table 2. Nominal chemical composition of the electrode ER5356 (% in weight)

Element	%Si	%Fe	%Cu	%Mn	%Mg	%Cr	%Zn	%Ti	%Al
ER5356	4.5-6.0	0.80	0.30	0.05	0.05	….	0.10	0.20	Rest

The chemical composition of the Aluminum alloy was determined by using an atomic absortion electro-photometer, Varia brand, model: AA-275 Serie, and are shown in Table 3.

Table 3. Nominal chemical composition of Aluminum alloy 6063 (% in weight)

Element	%Si	%Fe	%Cu	%Mn	%Mg	%Cr	%Zn	%Ti	%Al
Al 6063	0.2-0.6	0.35	0.10	0.10	0.45-0.90	0.10	0.10	0.20	Rest

Table 4, shows variation ranges for all the relevant parameters. Fifty four experiments resulted after combining four values of I, five E's and six V's.

Tabla 4. Electric current intensity, arc-voltage and welding speed

Intensity (Amperes)	150	180	210			
Voltage (Volts)	18	21	24			
Speed (cm/min)	50	59	68	77	86	95

The welding process was automated by using a MIG weld gun, brand Hobart with incorporated wire web, attached to a pantograph, brand Messer Grieheim GMBH. This arrangements permitted to maintain the arclength constant throughout all the trajectory.

A steel support plate for the aluminum probes was used to hold in place the aluminum plate while welding.

Each welding joint provided three samples obtained through the 15-milimiter longitudinal cut at the uniform region of the weld.

Numerical Simulation

The transient energy equation was solved using a finite-volume-based code (CFX4.2™). The optimal time-step was set up to obtain an acceptable convergence. The computation of gross or integral quantities (i.e., weld penetration and width) and the introduction of temperature-dependent physical properties (i.e., K(T) and Cp(T)), required the creation and validation of Fortran subroutines [6]. The mesh-independence of computational results was verified and afterwards, the final computational domain consisted of 80.000 regular control volumes. A Pentium III, 450 MHz-192 MB ram PC ran every simulation in 60 min. Average.

The process efficiency, η, was adjusted to obtain best fit in weld penetration and width between the numerical model and experiments [1]. Table 5, depicts final results after obtaining η.

Tabla 5. Comparison between experiments and numerical simulation

Pexp y Aexp: Experimental weld penetration and width, respectively (mm) Pcal y Acal: Computed weld penetration and width, respectively (mm) Err % (P) y Err % (A): Percent error for each of above parameters, related to experiments								
E = 18 V			I = 210 A		r_b = 3 mm			
V (cm/min)	Pexp		Pcal	Err % (P)	Aexp		Acal	Err %(A)
50 (η = 0.6)	2.81±0.39		2.858		8.81±0.13		6.668	
59 (η = 0.6)	2.27±0.33		2.646		7.84±0.14		6.668	
68 (η = 0.6)	1.99±0.29		2.434		8.31±0.17		6.032	
E = 21 V			I = 210 A		r_b = 3 mm			
V (cm/min)	Pexp		Pcal	Err % (P)	Aexp		Acal	Err %(A)
50 (η = 0.6)	3.97±0.34		3.493		10.79±0.06		7.938	
59 (η = 0.6)	2.76±0.43		3.281		9.37±0.23		7.302	
68 (η = 0.6)	1.97±0.11		3.069		9.11±0.17		7.302	
E = 24 V			I = 210 A		r_b = 3 mm			

V (cm/min)	Pexp		Pcal	Err % (P)	Aexp		Acal	Err %(A)
50 (η = 0.5)	4.51±0.33		3.281		12.71±0.08		7.302	
59 (η = 0.5)	2.75±0.25		3.069		10.78±0.50		7.302	
68 (η = 0.5)	3.01±0.36		2.858		9.93±0.21		6.668	

Tabla 6. Constants used in simulations

Tliq = 652 ºC
Tsol = 582 ºC
Tinf = 22 ºC
Density (ρ) = 2700 kg/m^3
Emisivity (ε) = 0.9

CONCLUDING REMARKS

The plate-to-plate arc-buttwelding process is modeled and simulated using a finite volume numerical solver. Computed results are validated against experimental data, demonstrating excellent agreement. The model validation included the calibration of the process efficiency.

The maximum difference, between computed results and experiments, found in the heat penetration was 6.75%. However, the computed weld width did present differences up to 30% with experiments. The difference is believed to obey to the lack of melting material dropping onto the substrate in the model, as it does occur in experiments.

This report is a preliminary work to build a more robust and realistic mathematical model to simulate the highly complex two-plate butt arc-welding process, thus further investigation is currently ongoing in that direction.

REFERENCES

1. Payares, C,. *Modelo para la Determinación de la Penetración e Influencia de los Parámetros de Operación en la Geometría del Cordón en Soldaduras a Tope de Aluminio 6063 T5*, Trabajo de Ascenso (Universidad Simón Bolívar), Caracas, 1985
2. T. J. Lho, S. J. Na,. A Study on Three-Dimensional Transient Heat Flow in Circumferential GTA Welding of Pipes Using Periodicity Conditions, *Journal of Engineering of Manufacture*, Vol. 205(B4): 271-278, 1991
3. J. Goldak, A. Chakravarti, M, Bibby,. A New Finite Element Model for Welding Heat Sources, *Metallurgical Transactions B*, Vol. 15B: 299-305, 1984
4. S. J. Na, S. Y. Lee,. A Study on Three-Dimensional Analysis of the Transient Temperature Distribution in Gas Tungsten Arc, *Journal of Engineering of Manufacture*, Vol. 201(B3): 149-156, 1987
5. E. Pardo, D.C. Weckman,. Prediction of Weld Pool and Reinforcement Dimensions of GMA Welds Using a Finite Element Model, *Metallurgical Transactions B*, Vol. 20B: 937-947, 1989
6. AEA Technology,. CFX 4.2 Solver Manual, 1997